dwarf virus isolates from different hosts reveal low genetic diversity within the wheat strain. *Plant Pathol.*, 2008, **57**, 834–841.

8. Zhang, X., Zhou, G. and Wang, X., Detection of wheat dwarf virus (WDV) in wheat and vector leafhopper (*Psammotettix alienus* Dahlb.) by real-time PCR. *J. Virol. Methods*, 2010, **169**, 416–419.

9. Kumar, J., Kumar, A., Roy, J. K., Tuli, R. and Khan, J. A., Identification and molecular characterization of begomovirus and associated satellite DNA molecules infecting *Cyamopsis tetragonoloba*. *Virus Genes*, 2010, **41**, 118–125.

10. Singh, S. P. *et al.*, Pattern of iron distribution in maternal and filial tissues in wheat grains with contrasting levels of iron. *J. Exp. Bot.*, 2013, **64**, 3249–3260.

Magnetic fabric studies of sandstone from Jhuran Formation (Kimmeridgian–Tithonian) of Jara dome, Kachchh Basin, northwest India

V. Periasamy and M. Venkateshwarlu*

CSIR-National Geophysical Research Institute, Uppal Road, Hyderabad 500 007, India

Low-field anisotropy of magnetic susceptibility (AMS) study was performed on the clastic sandstones of the Jhuran Formation from the Jara dome in the Kachchh basin. The AMS results consistent with petrographic analysis indicate primary deposition fabric for Arkose, sub-litharenite, wacke and quartz arenite sandstones of the Jhuran Formation. Isothermal remanent magnetization and thermal demagnetization curves indicate that magnetite, titano-magnetite and hematite are the chief magnetic minerals contributing to the AMS. The distribution of K_1, K_2 and K_3 axes in the stereographic projections suggest depositional fabric development for arkose, sub-litharenite and wacke, whereas dispersed K_3 axes for quartz arenite are inferred to be due to low strain activity. The shape factors *T*, *q* confirm the oblate-shaped ellipsoid and horizontal fabric respectively, for all samples. The reconstructed palaeoflow directions for arkose and sub-litharenite are NW–SE and for wacke and quartz arenite are NE–SW based on K_1 AMS axis.

Keywords: AMS, magnetic fabric, Kachchh basin, palaeoflow directions.

IN clastic sedimentary rocks, magnetic fabric is produced during physical transportation and deposition of magnetic particles. Studies of the magnetic fabric provide information concerning palaeoflow directions, environment of deposition, influence of tectonism and weak deformation of rock units[1–3]. The low-field anisotropy of magnetic susceptibility (AMS) is a widely used technique to determine the magnetic fabric and palaeoflow direction of the sediments and sedimentary rocks, particularly sandstone. Generally the shape of the magnetic susceptibility ellipsoids provides insight into the mode of deposition, i.e. in still water, the minimum susceptibility axes of the grains are clustered on the pole, while the maximum and intermediate axes disperse uniformly on the bedding plane. Whereas the flowing water current results in the alignment of susceptibility axes which lie in different directions[4–8].

This communication presents AMS results of sandstone of the Upper Jurassic (Kimmeridgian to Tithonian) Jhuran Formation exposed in Jara dome in the Kachchh sedimentary basin.

The Kachchh basin is located in western India (Figure 1). Formation of the basin is linked to the break-up between eastern and western Gondwanaland during Late Triassic/Early Jurassic period[9–11]. The rift basin contains several intra-basinal strike faults such as the Island Belt Fault (IBF), the Banni Fault (BF), the Kachchh Mainland Fault (KMF), the Katrol Hill Fault (KHF) and the South Wagad Fault (SWF). A first-order meridional (NNE–SSW) high is found across the middle of the basin[12].

The basin consists of 2000–3000 m thick Mesozoic sediments ranging in age from Lower Jurassic to Lower Cretaceous, 600 m of Tertiary sediments and a thin sheet of Quaternary sediments. The rock outcrops are better exposed in the uplifted regions of the basin, such as Kachchh Mainland, Pachham Island, Khadir Island, Bela Island, Chorar Island and Wagad uplifts. Lower Jurassic to Lower Cretaceous are well preserved in the Kachchh Mainland. The stratigraphic succession of Kachchh Mainland is divided into four formations, namely Jhurio (Bathonian to Callovian), Jumara (Callovian to Oxfordian), Jhuran (Kimmeridgian to Lower Cretaceous) and Bhuj (pre-Aptian to Santonian (?)) Formations in ascending stratigraphic order[13], are best exposed in a series of domes at Habo, Jhura, Keera, Nara, Jumara and Jara hills (Figure 1). The lithological sequence of these formations consists of clastic sandstone, siltstone, shale and limestone with distinct demarcation boundary, deposited in marine to fluviodeltaic conditions.

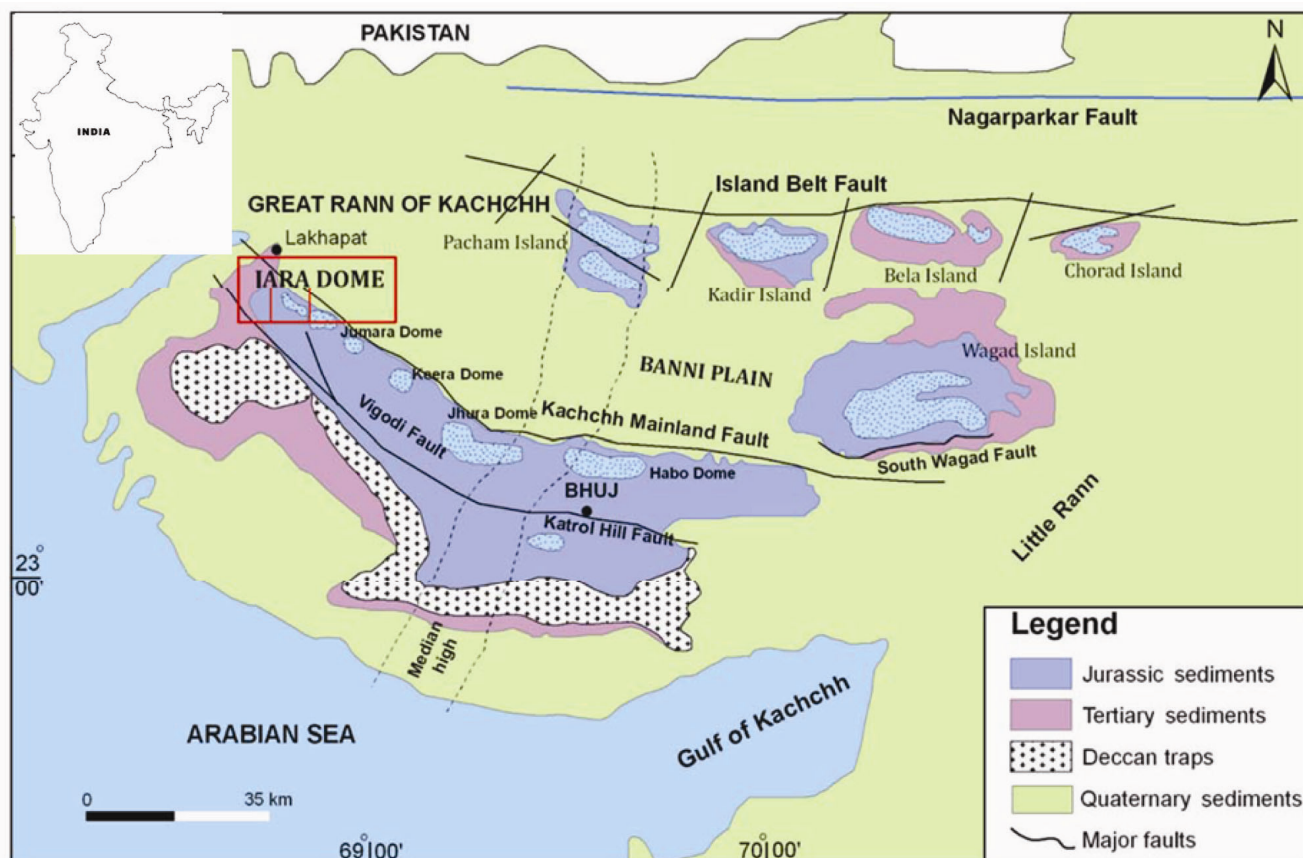*For correspondence. (e-mail: mamila_v@rediffmail.com)

Figure 1. Simplified geological map with major structural features of Kachchh basin showing the study area, Jara dome (red rectangle; modified after Wynne[24]).

The Jara dome is situated on the western fringe of the Mainland Kachchh where the Jumara, Jhuran and Bhuj formations are best exposed. The lithostratigraphic sequence of Jhuran Formation in Jara dome containing alternating beds of sandstone and shale stratigraphically overlies the Jumara formation (Figure 2). The study area covers ~500 m thick sediments belonging to Lower and Middle members of the Jhuran Formation. The Lower members include shale, siltstone, yellow and red sandstone and the Middle members include shale with ferruginous sandstone beds.

Figure 3 shows photomicrographs of sandstones of Jhuran Formation. Petrographically the sandstones are fine-grained, sometimes medium to coarse-grained, poor to moderately sorted with fair amount of matrix. Quartz, K-feldspar, plagioclase, lithic fragments and detrital grains are present. Quartz is subrounded to subangular with mechanical fractures. Monocrystalline quartz (87%) dominates over polycrystalline quartz (1.62%) showing straight to strong undulose extinction. K-feldspar (mostly microcline with cross-hatched twinning; 4.5%) and plagioclase (1%) are subrounded to subangular, Chert constitutes the predominant lithic fragments (Figure 3 *a*). The matrix (2% to 15%) is of both calcareous and

ferruginous nature (Figure 3 *a–c*). Opaque minerals include magnetite, hematite and titano-magnetite. Zircon is observed as an accessory phase. Figure 3 *d* shows the detrital titano-magnetite grain seen in the arkose sandstone.

A total of 35 oriented block samples were collected from the outcrops of Jhuran Formation (only from Lower and Middle members) exposed in the Jara dome. The samples were collected from the horizontal beds of siliclastic sedimentary rocks, i.e. sandstones covering ~500 m thickness. All the samples were drilled and cut into standard specimens (2.2 cm length and 2.5 cm diameter). Ninety specimens were selected (21 arkose, 19 sub-litharenite, 15 wackes and 12 quartz arenite were used) for AMS and bulk susceptibility measurements. AMS measurements were done in 15 different directions using Kappa Bridge MFK1-FA (Brno, Czech Republic) susceptibility meter following the standard methods described by Jelinek[14]. AMS results from 23 specimens (out of 90) were discarded due to their scattered nature.

The AMS parameters measured in this study are given in Table 1. The magnetic susceptibility (K) of the rock sample is obtained when it is subjected to induced magnetization (J) by an applied field (H) following the formula $J = kH$. The mean susceptibility (K_m) is calculated
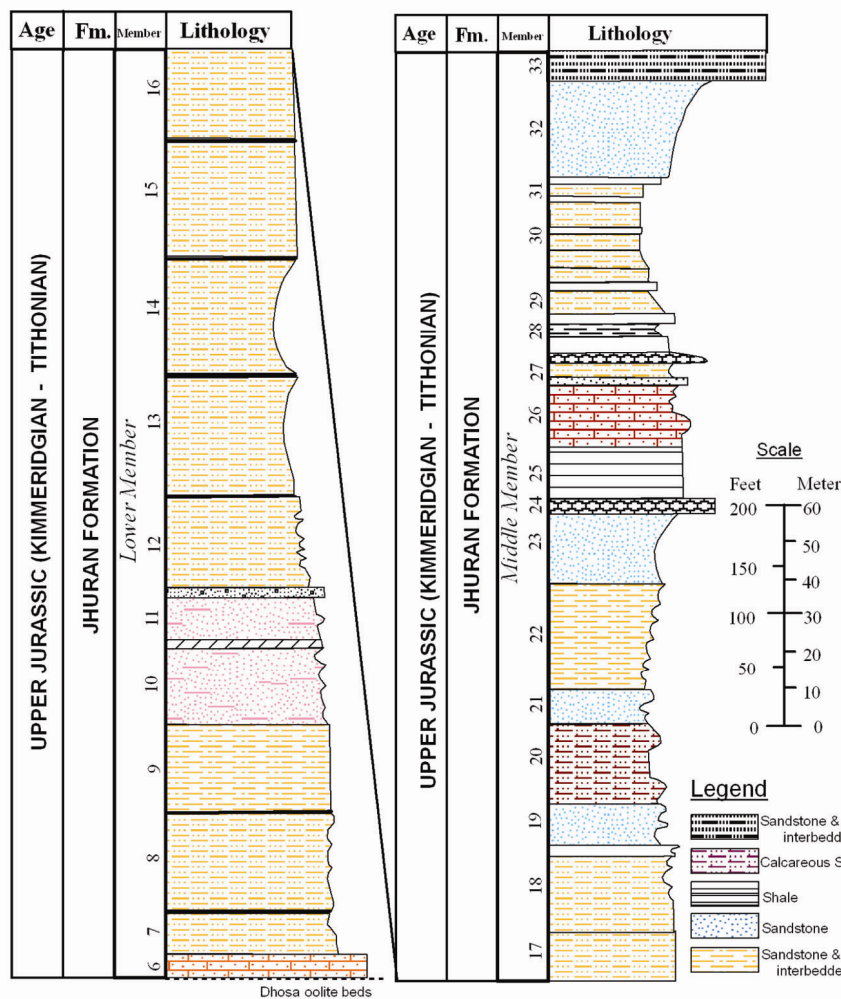
Figure 2. Studied lithostratigraphic sequence of Lower and Middle members of Jhuran formation, Jara dome.

Table 1. Anisotropy of magnetic susceptibility (AMS) parameters measured in this study

Parameter	Formula	Reference
Mean susceptibility	$K_m = (K_1 + K_2 + K_3)/3$	16
Foliation	$F = K_2/K_3$	15
Lineation	$L = K_1/K_2$	25
Shape factor	$T = (2\eta_2 - \eta_1 - \eta_3)/(\eta_1 - \eta_3)$	19
q-factor	$q = (K_1 - K_2)/(0.5(K_1 + K_2) - K_3)$	18
Corrected anisotropy degree	$P_j = \exp\sqrt{2[(\eta_1 - \eta_m)^2 + (\eta_2 - \eta_m)^2 + (\eta_3 - \eta_m)^2]}$	19
	where $\eta_1 =$ in K_1, $\eta_2 =$ in K_2; $\eta_3 =$ in K_3; $\eta_m = \sqrt[3]{\eta_1 \cdot \eta_2 \cdot \eta_3}$	

K_1, Maximum; K_2, intermediate; K_3, minimum susceptibility axes.

by the formula $K_m = (K_1 + K_2 + K_3)/3$ where K_1, K_2 and K_3 are the maximum, intermediate and minimum susceptibility axes respectively[14]. The directions of the susceptibility axes are presented on the lower hemisphere of the equal area projection. The magnetic foliation (F) is developed when the magnetic particles or platy minerals are arranged with their shortest and longest AMS axes perpendicular and parallel to the bedding plane respectively.

The lineation (L) is developed when the K_{max} axes of particles are arranged parallel to the water current; however, perpendicular or oblique arrangements are also common. F and L are obtained using the formula $F = K_2/K_3$ and $L = K_1/K_2$ respectively[14,15].

Generally, two shape parameters T ($-1 \geq T \geq 1$) are known for the susceptibility ellipsoids. When $T < 0$, the shape of the ellipsoid is prolate (rod-shaped), and when
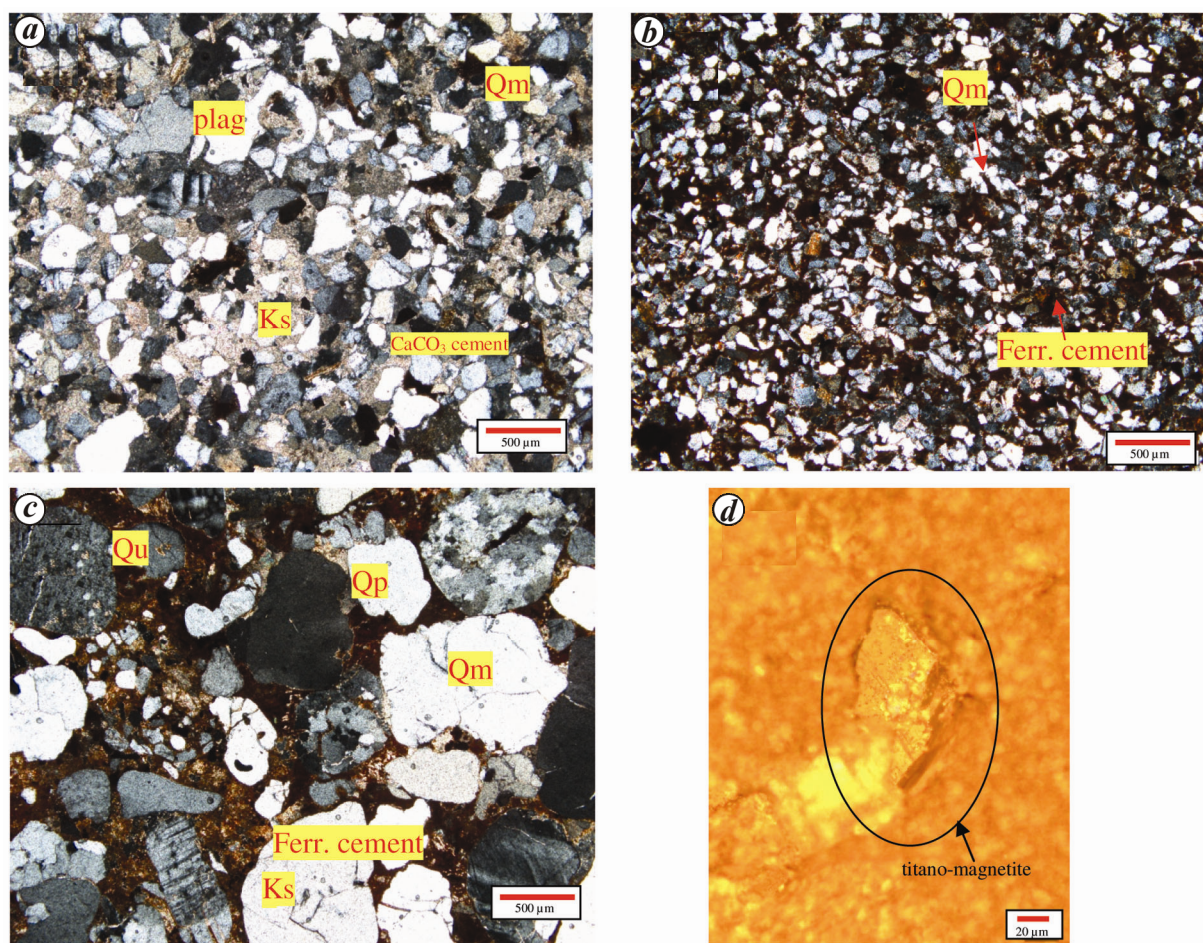
Figure 3. Photomicrographs of sandstones from Jhuran formation. *a*, Arkosic sandstone with subrounded monocrystalline quartz (Qm), K-feldspar (Ks) and plagioclase (plag) minerals cemented by carbonate matrix. *b*, Wacke sandstone containing largely monocrystalline quartz (Qm) cemented by ferruginous cement. *c*, Quartz arenite with monocrystalline quartz (Qm), polycrystalline quartz (Qp), undulose quartz (Qu), K-feldspar (Ks) and iron cement. *d*, Arkose sandstone showing titano-magnetite grain under reflected microscope.

$T > 0$, the ellipsoid is oblate (disc-shaped) and it is calculated by $T = (2\eta_2 - \eta_1 - \eta_3)/(\eta_1 - \eta_3)$, where $\eta_1 = $ in K_1; $\eta_2 = $ in K_2; $\eta_3 = $ in K_3 (ref. 16). The other parameter is called q-factor, which is commonly used to distinguish the nature of fabric development, viz. either depositional or tectonic fabric[17]. Usually $q = (K_1 - K_2)/(0.5(K_1 + K_2) - K_3)$ after Granar[18] ranging between 0.06 and 0.7 indicates primary depositional fabric, and $q > 0.7$ indicates tectonic fabrics. The eccentricity and shape of susceptibility ellipsoid are represented graphically by a Flinn plot, in which magnetic foliation (F) and magnetic lineation (L) are plotted on the x and y axis respectively. Additionally, the degree of anisotropy is obtained by $P_j = \exp\sqrt{2[(\eta_1 - \eta_m)^2 + (\eta_2 - \eta_m)^2 + (\eta_3 - \eta_m)^2]}$ after Jelinek[19], which is used to describe the degree to which the ellipsoid is oblate or prolate.

Bulk susceptibility of the samples ranges from 3.33×10^{-5} to 8.5×10^{-4} SI (average value of 1.65×10^{-4} SI). Figure 4 shows the isothermal remanent magnetization (IRM) acquisition curves obtained using MMPM 10

(Magnetic Measurements, UK) pulse magnetizer. The curves show that the magnetization fields are not saturated till 3T of applied magnetic field. On the other hand, the IRM results reflect the differences in magnetic mineralogy and grain size of magnetic minerals present in the sediment. A steep initial increase up to 300 mT is observed for all samples indicates dominance of low-coercivity magnetic phases like magnetite and maghaemite. Samples 2.1AII and 15.3CII demonstrates a high-coercivity phase such as hematite at 150–300 mT after which a gradual rise is observed till 3T. However, thermal demagnetization study on selected samples shows the dominance of low coercive force magnetic minerals in the studied samples. Overall the investigated samples are dominated by low coercive mineral, i.e. goethite with an appreciable amount of magnetite and hematite mineral assemblage.

Table 2 gives the results of AMS parameters obtained from this study. The average mean bulk magnetic susceptibility (K_m) for arkose, sub-litharenite, wacke and quartz arenite samples are 1.31×10^{-4}, 1.55×10^{-4}, 2.30×10^{-4}

Table 2. Data of AMS parameters obtained from sandstones of Jhuran formation, Kachchh basin

Lithology	n = No. of specimens	K_m	K_1		K_2		K_3		L	F	P_j	T	q
			D	I	D	I	D	I					
Arkose	21	1.16×10^{-05}	69.3	2.1	339.2	3.2	192.3	86.1	1.015	1.044	1.064	0.405	0.09
Sub-litharenite	19	1.55×10^{-04}	65.3	7	155.9	4.2	276.6	81.9	1.01	1.025	1.036	0.421	0.22
Wacke	15	2.30×10^{-04}	149.7	6.7	59.7	0.3	327.4	83.3	1.013	1.022	1.037	0.359	0.15
Quartz arenite	12	2.08×10^{-04}	271.1	4.6	1.6	6	143.6	82.4	1.012	1.017	1.029	0.07	0.53

K_m, Bulk magnetic susceptibility; K_1, K_2, K_3, Maximum, intermediate and minimum susceptibility axes respectively; D and I, Declination and inclination; L, Magnetic lineation; F, Magnetic foliation; P_j, Degree of anisotropy; T and q, Magnetic ellipsoid shape factors.
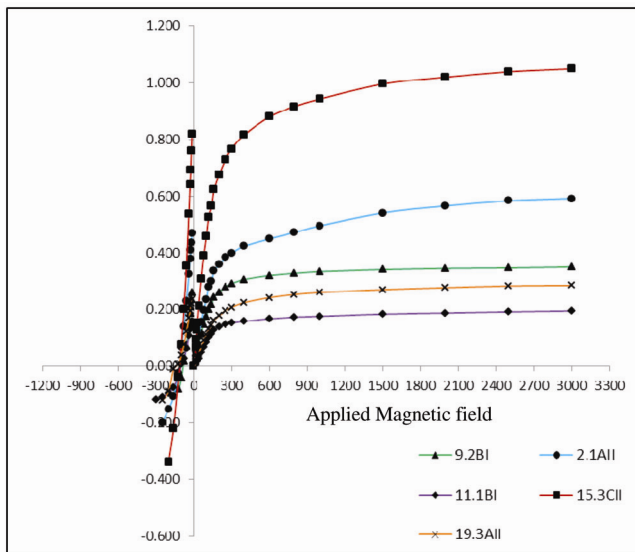

Figure 4. IRM acquisition curves obtained from arkose, sub-litharenite, wacke and quartz arenite sandstone samples of Jhuran formation.

and 2.08×10^{-4} SI units respectively (Table 2). The uneven bulk magnetic susceptibility values in the Jhuran sandstones can be attributed to their variable grain size and presence of more than one phase of magnetic minerals. Figure 5 is the Flinn diagram derived by plotting L against F, which displays the frequency distribution of K_m. It can be clearly noted that K_m is mainly controlled by grain size variation, i.e. wacke samples have high K_m while arkose, sub-litharenite and quartz arenite show low magnetic lineation and foliation values L = ~1.01; F = ~1.02. The Flinn diagram shows oblate-shaped fabric for all sandstone types with few samples plotted in prolate-shaped field.

Figure 6 shows the equal area stereographic projections for four varieties of sandstones. The figure shows the primary sedimentary fabrics with K_3 (minimum) axis clustered on the pole, while the K_1 (maximum) and K_2 (intermediate) axes dispersed on the horizontal plane. Furthermore, wacke sandstone demonstrates excellent grouping of K_3 axis due to its fine-grained nature, which resulted in a fine compaction compared to other coarser sandstones (Figure 6 c). The degree of anisotropy (P_j) of

the studied samples varies from 1.013 to 1.132 (arkose), 1.004 to 1.098 (sub-litharenite), 1.012 to 1.095 (wacke) and 1.009 to 1.06 (quartz arenite), with the average values of 1.064, 1.035, 1.037 and 1.029 respectively. The relatively high value of P_j is seen in arkose samples can be attributed to the existence of magnetite mineral which is consistent with petrographic observation (Figure 3 d). The plot of T against P_j in Figure 6 a1, b1, c1 and d1 also confirms the oblate-shaped AMS ellipsoid. The shape factor T obtained from Jhuran sandstones shows strong oblate fabrics with T value greater than 0.1 for all sandstone types; however, few samples show prolate-shaped fabric (Table 2). Another shape parameter q exhibits values of 0.08, 0.22, 0.15 and 0.53 for arkose, sub-lithararenite, wacke and quartz arenite respectively, suggestive of undeformed primary fabrics in the studied samples (Table 2).

This study shows that the AMS analysis consistent with petrographic investigation in sediments is a useful method to understand the processes associated with the development of magnetic fabric and its palaeoflow directions, in particular, sandstones. IRM and thermal demagnetization techniques are used in this study to identify the magnetic minerals contributing to the total AMS. The results of these methods indicate the occurrence of low-coercive minerals such as goethite, magnetite and titanomagnetite with fair amount of hematite in the examined samples. The AMS axes (K_1, K_2 and K_3) of the sandstones from Jhuran formation plotted on equal area stereographic projection reflect the primary depositional fabric (Figure 6). The mechanism of formation of primary sedimentary fabric by means of the long and intermediate AMS axis lie parallel to the bedding plane whereas the short one deposit perpendicular to the bedding plane[1]. From this result, it can be deduced that the sediments of the Jhuran formation deposited in still water with slight water current and also by gravity settling process.

In general, the fine-grained sedimentary rocks show clear foliation plane than coarser ones. The observation of AMS axis in the stereographic projection proves that the wacke sandstone has well-defined foliation plane as seen that the K_3 axis clustered well on the pole (Figure 6 c) than the arkose, sub-litharenite and quartz arenite samples where the K_3 axis is dispersed (Figure 6 a, b and d). Also,
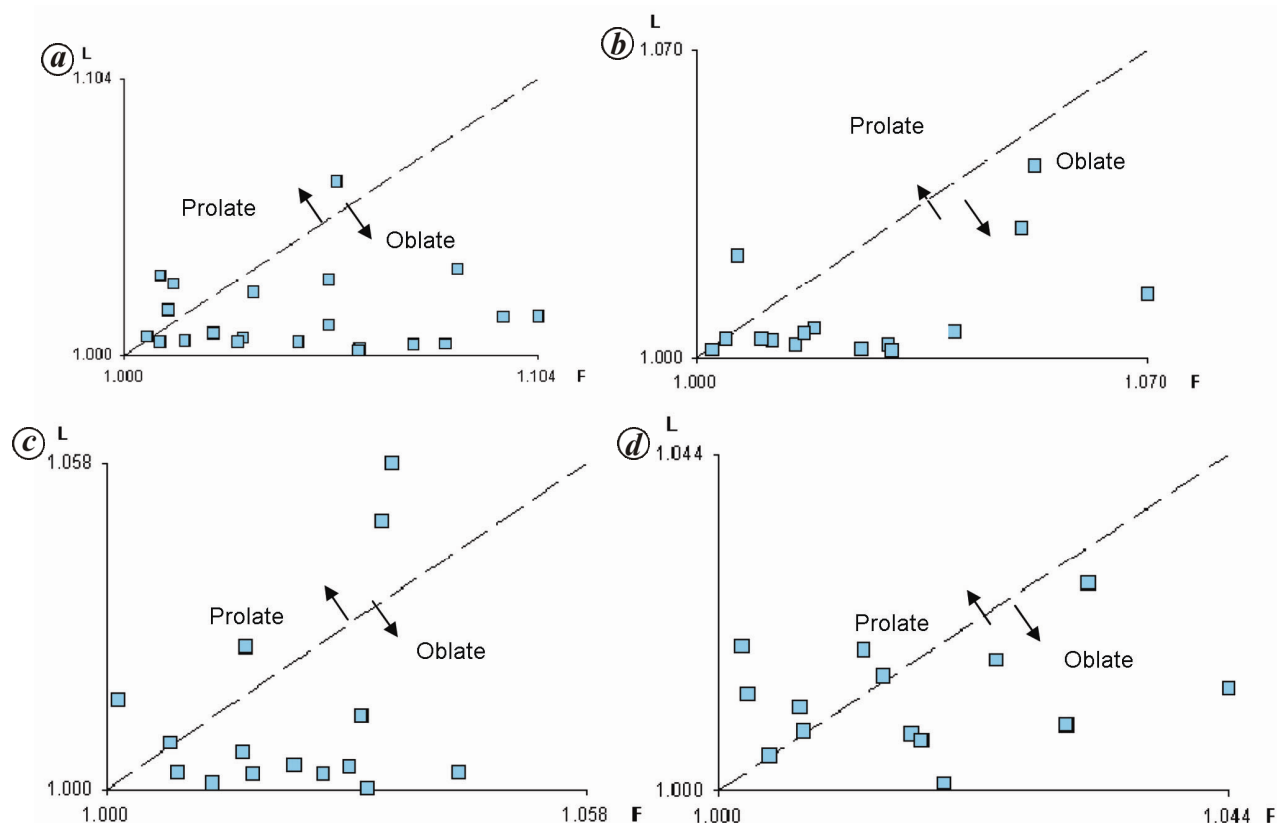
Figure 5. Flinn diagram of *F* (magnetic foliation) against *L* (magnetic lineation) plot for (***a***) Arkose, (***b***) sub-litharenite, (***c***) wacke and (***d***) quartz arenite in oblate-shaped ellipsoid field.

except wacke, other sandstones show slight to moderate imbrications which could be attributed to changing strength of water current and direction. Among the four sandstone types, the AMS axis of quartz arenite is more scattered which can be attributed to its coarseness (Figure 6 *d*), because deposition of coarse grains occurs during high energy environment which can influence the preferred orientation of ferromagnetic and paramagnetic minerals contributing to AMS.

The shape factor *T* value above 0.1 for arkose, sub-litharenite and wacke shows strong oblate fabric whereas quartz arenite indicates slight prolate nature with a *T* value of 0.076, suggesting that a slight strain occurred during deposition (Table 2). The *q* value for all samples varied between 0.06 and 0.7, which supports undeformed primary sedimentary fabric (Table 2). It is further supported by the plots of *L* versus *F* and *T* versus P_j, wherein the greater part of measured samples falls in oblate-shaped AMS ellipsoid fields with slight prolate-shaped development (Figures 5 and 6 *a*1, *b*1, *c*1 and *d*1).

Although the Kachchh basin has undergone prominent tectonic disturbances, absence of lineation is observed in all sandstones indicating that the tectonic disturbances have very little influence on the studied samples. Usually compaction (post-depositional) increases the oblateness of susceptibility ellipsoid with depth as a result of compression by overlying sediment layers[6,20,21]; however, the

samples of Jhuran sandstones show absence or very little compaction effect as the axes are not changed significantly within the beds of the studied stratigraphic column.

In general, it is difficult to establish the exact direction of flow from horizontal primary sedimentary fabric because the long axis deposit randomly in any direction on the bedding plane. However, numerous primary sedimentary structures have been studied to identify the palaeoflow directions of the siliclastic rocks of the Jhuran formation and its overlying rocks[22,23]. The available data on the sedimentary structures (such as ripple marks, cross-bedding and groove casts) indicate that the palaeocurrent directions of the Jhuran sandstones were NW–SE to NE–SW. In this study, it is observed that the K_1 axis of the AMS ellipsoid lies parallel to the flow direction which is consistent with the *in situ* measurements of the above-mentioned sedimentary palaeocurrent indicators. Figure 7 shows the rose diagram derived from declination and inclination of K_1 axis as an indicator of palaeoflow direction. The established palaeocurrent direction from this AMS study for arkose and sub-litharenite is NW–SE (Figure 7 *a* and *b*), while wacke and quartz arenite show NE–SW directions (Figure 7 *c* and *d*).

Thermal demagnetization and IRM study revealed that the primary magnetic minerals which control the AMS fabric are goethite, magnetite, titano-magnetite and considerable amount of hematite. The value of bulk magnetic
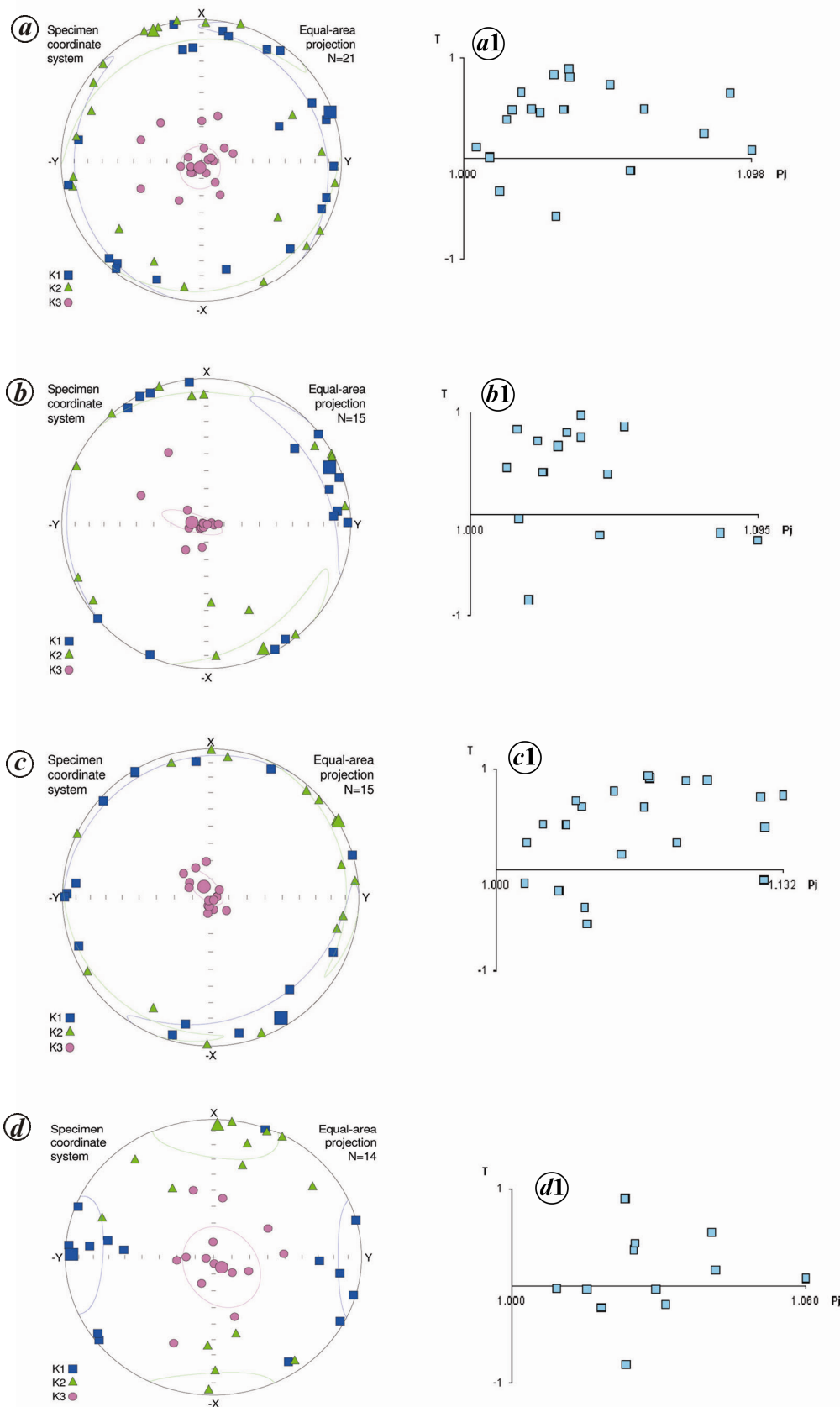
Figure 6. Equal area stereographic projection demonstrates the distribution of K_{min}, K_{int} and K_{max} axes in the analysed samples: (**a**) arkose, (**b**) sub-litharenite, (**c**) wacke and (**d**) quartz arenite. Plot of T against P_j is shown in **a1**, **b1**, **c1** and **d1**.
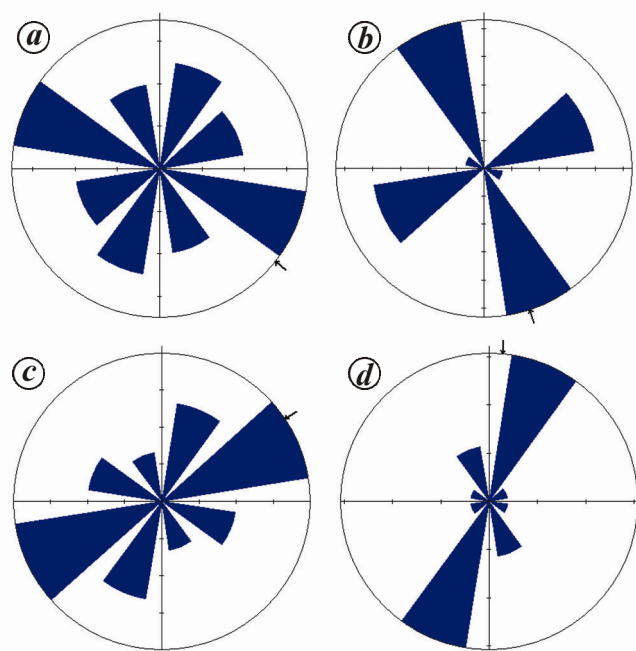
Figure 7. Rose diagram derived from K_1 (declination and inclination values) axis as an indicator of palaeoflow directions for (**a**) arkose, (**b**) sub-litharenite, (**c**) wacke and (**d**) quartz arenite.

susceptibility indicated the presence of small amounts of paramagnetic minerals. Based on petrographic analysis, the sandstones of the Jhuran formation have been classified into arkose, sublitharenite, wacke and quartz arenite. The magnetic fabric of the studied formation indicates the primary depositional fabric which developed in low-velocity water current. The palaeocurrent direction recorded in arkose and sub-litharenite is NW–SE, whereas in wacke and quartz arenite it is NE–SW direction. The overall flow direction is from NW to SE with significant changes in the path during the time of deposition of the entire sedimentary sequences. Further detailed study regarding the separation of individual magnetic minerals contributing to the total AMS is essential for greater understanding.

1. Tarling, D. H. and Hrouda, F., *The Magnetic Anisotropy of Rocks*, Chapman and Hall, London, 1993, p. 213.
2. Borradaile, G. J. and Henry, B., Tectonic application of magnetic susceptibility and its anisotropy. *Earth Sci. Rev.*, 1997, **42**, 49–93.
3. Baas, J. H., Hailwood, E. A., McCaffrey, W. D., Kay, M. and Jones, R., Directional petrological characterization of deep-marine sandstones using grain fabric and permeability anisotropy: methodologies, theory, application and suggestions for integration. *Earth Sci. Rev.*, 2007, **82**, 101–142.
4. Rees, A. I., The use of anisotropy of magnetic susceptibility in the estimation of sedimentary fabric. *Sedimentology*, 1965, **4**, 257–271.
5. Ellwood, B. B., Application of the anisotropy of magnetic susceptibility method as a indicator of bottom water flow direction. *Mar. Geol.*, 1980, **34**, 83–90.
6. Hrouda, F., Magnetic anisotropy of rocks and its application in geology and geophysics. *Geophys. Surv.*, 1982, **5**, 37–82.
7. Lowrie, W. and Hirt, A. M., Anisotropy of magnetic susceptibility in the Scaglia Rossa pelagic limestone. *Earth Planet. Sci. Lett.*, 1987, **82**, 349–356.
8. Veloso, E. E., Anma, R., Ota, T., Komiya, T., Kagashima, S. and Yamazaki, T., Paleocurrent patterns of the sedimentary sequence of the taitao ophiolite constrained by anisotropy of magnetic susceptibility and paleomagnetic analyses. *Sediment. Geol.*, 2007, **201**, 446–460.
9. Norton, I. O. and Sclater, J. G., A model for the evolution of the Indian Ocean and the breakup of Gondwanaland. *J. Geophys. Res. B*, 1979, **84**(12), 6803–6830.
10. Biswas, S. K., Regional tectonic framework, structure and evolution of India, with special reference to western margin basins of India. *Tectonophysics*, 1987, **135**, 307–327.
11. Biswas, S. K., A review of structure and tectonics of Kutch basin, western India, with special reference to earthquakes. *Curr. Sci.*, 2005, **88**, 1592–1600.
12. Biswas, S. K., Mesozoic rock stratigraphy of Kutch. *Q. J. Geol., Min., Metal. Soc. India*, 1977, **49**, 1–52.
13. Kanjilal, S. and Prasad, S., Geology and stratigraphy of the Callovian–Oxfordian (Jurassic) rocks of Jara Dome, District Kachchh, Gujarat, W. India. *J. Indian Acad. Geosci.*, 1992, **35**(1), 1–18.
14. Jelinek, V., Statistical processing of anisotropy of magnetic susceptibility measured on groups of specimens. *Stud. Geophys. Geodet.*, 1978, **22**, 50–62.
15. Stacey, F. D., Joplin, G. and Lindsay, J., Magnetic anisotropy and fabric of some foliated rocks from SE Australia. *Geophysica Pura. Appl.*, 1960, **47**, 30–40.
16. Nagata, T., *Rock Magnetism*, Maruzen, Tokyo, 1961, 2nd edn, p. 350.
17. Hamilton, N. and Rees, A. I., The use of magnetic fabric in palaeocurrent estimation. In *Palaeogeophysics* (ed. Runcorn, S. K.), Academic Press, London, 1970, pp. 445–464.
18. Granar, L., Magnetic measurements on Swedish varved sediments. *Ark. Geophys.*, 1958, **3**, 1–40.
19. Jelinek, V., Characterization of the magnetic fabric of rocks. *Tectonophysics*, 1981, **79**, 63–67.
20. Graham, J. W., Significance of magnetic anisotropy in Appalachian Sedimentary rocks. In *The Earth Beneath the Continents*, Geophys. Monograms, Washington DC, 1966, pp. 627–648.
21. Ellwood, B. B., Bioturbation: minimal effects on the magnetic fabric of some natural and experimental sediments. *Earth Planet. Sci. Lett.*, 1984, **67**, 367–376.
22. Balagopal, A. T. and Saha, Ajit Kumar, Sedimentary structures in the Jurassic rocks of Central Kutch, Gujarat. *Proc. Indian Natl. Sci. Acad.*, 1974, **40**, 320–330.
23. Shukla, U. K. and Singh, I. B., Facies analysis of Bhuj sandstone (Lower Cretaceous) Bhuj area, Kachchh. *J. Paleontol. Soc. India*, 1990, **35**, 189–196.
24. Wynne, A. B., Memoir on the Geology of Kutch to accompany the map compiled by A.B. Wynne and F. Fidden during the season of 1867–1868 and 1868–1869. *Mem. Geol. Surv. India*, 1872, **9**(1), 1–293.
25. Balsley, J. R. and Buddington, A. F., Magnetic susceptibility, anisotropy and fabric of some Adirondack granites and orthogneisses. *Am. J. Sci. A*, 1960, **258**, 6–20.